Journal of Molecular Structure 1075 (2014) 254–263

Contents lists available at ScienceDirect

Journal of Molecular Structure

journal homepage: www.elsevier.com/locate/molstruc

Synthesis, characterization, electrochemical studies and DFT calculations of amino acids ternary complexes of copper (II) with isonitrosoacetophenone. Biological activities

Nabila Tidjani-Rahmouni [a], Nour el Houda Bensiradj [b], Safia Djebbar [a], Ouassini Benali-Baitich [a,*]

[a] Laboratoire d'Hydrométallurgie et Chimie Inorganique Moléculaire, Faculté de Chimie, USTHB, BP 32 El Alia, Bab Ezzouar, Alger, Algeria
[b] Laboratoire de Chimie Théorique Computationnelle et Photonique, Faculté de Chimie, USTHB, BP 32 El Alia, Alger, Algeria

HIGHLIGHTS

- Copper complexes containing amino acids and oxime have been characterized.
- A distorted octahedral geometry has been conjectured from DFT calculations.
- The electrochemical behavior was determined by cyclic voltammetry.
- The complexes show a good antifungal activity.
- Antioxidant activity for these complexes has been evaluated.

GRAPHICAL ABSTRACT

The optimized structure of $[Cu(INAP)(Hist)(H_2O)_2]$.

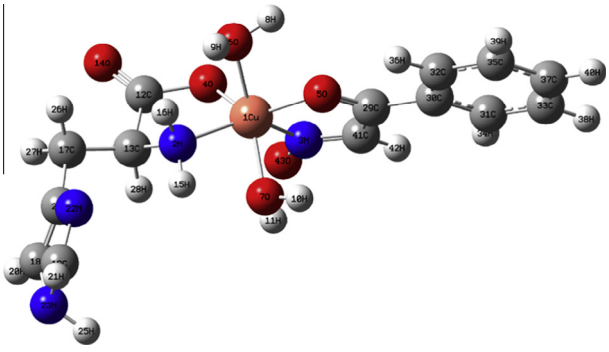

ARTICLE INFO

Article history:
Received 21 March 2014
Received in revised form 29 May 2014
Accepted 23 June 2014
Available online 3 July 2014

Keywords:
Ternary complexes
Isonitrosoacetophenone
Amino acids
ESR spectroscopy
Cyclic voltammetry
Biological activity

ABSTRACT

Three mixed complexes having formula $[Cu(INAP)L(H_2O)_2]$ where INAP = deprotonated isonitrosoacetophenone and L = deprotonated amino acid such as histidine, phenylalanine and tryptophan have been synthesized. They have also been characterized using elemental analyses, molar conductance, UV–Vis, IR and ESR spectra. The value of molar conductance indicates them to be non-electrolytes. The spectral studies support the binding of the ligands with two N and two O donor sites to the copper (II) ion, giving an arrangement of N_2O_2 donor groups. Density Functional Theory (DFT) calculations were applied to evaluate the *cis* and *trans* coordination modes of the two water molecules. The *trans* form was shown to be energetically more stable than the *cis* one.

The ESR data indicate that the covalent character of the metal–ligand bonding in the copper (II) complexes increases on going from histidine to phenylalanine to tryptophan.

The electrochemical behavior of the copper (II) complexes was determined by cyclic voltammetry which shows that the chelate structure and electron donating effects of the ligands substituent are among the factors influencing the redox potentials of the complexes.

The antimicrobial activities of the complexes were evaluated against several pathogenic microorganisms to assess their antimicrobial potentials. The copper complexes were found to be more active against Gram-positive than Gram-negative bacteria.

* Corresponding author. Tel.: +213 776758928; fax: +213 21247311.
E-mail address: benali.baitich@gmail.com (O. Benali-Baitich).

http://dx.doi.org/10.1016/j.molstruc.2014.06.067
0022-2860/

Furthermore, the antioxidant efficiencies of the metal complexes were determined by 2,2-diphenyl-1-picrylhydrazyl (DPPH) radical scavenging activity. The antioxidant activity of the complexes indicates their moderate scavenging activity against the radical DPPH.

Introduction

Metal ions are currently known to be required for normal biological functions in humans. Among these metals, copper is one of many trace elements required for good health. It plays an important role in many biological oxidation–reduction reactions and is also a component of many proteins [1].

Copper complexes have attracted great deal of attention the last years due to their therapeutic applications as antimicrobial and antioxidant.

They have also been widely used in clinic applications as enzymes inhibitors [2], antiviral [3–5], antibacterial [6,7] and anticancer [8–12].

The variety of chemical structure of copper complexes gives a wide range of possibilities in synthesis of compounds with different specificities. Pharmacologic properties of complexes can depend on the properties of either metal or ligand or both [13].

The study of ternary complexes involving an oxime as the primary ligand, various amino acids as the secondary one can serve as useful models for gaining a better understanding of enzyme–metal-ion–substrate complexes, which play an important role in metalloenzyme catalysed biochemical reactions [14].

Ternary complexes of oxygen-donor ligands have attracted much interest as they can display exceptionally high stability.

Considerable attention has been paid to the chemistry of oximes which are becoming increasingly important as analytical and antimicrobial reagents.

Amino acids are essential building of many biological molecules and play key roles in several neurochemical response mechanisms, such as memory, appetite control and pain transmission [15].

Histidine is an essential amino acid and has a positively charged imidazole functional group. It is a precursor for histamine and carnosine biosynthesis [16,17]. Its imidazole side group containing two nitrogen atoms can participate in the metal–ligand coordination.

Phenylalanine is essential to many functions and is one of the few amino acids that can directly affect brain chemistry by crossing the blood–brain barrier [18].

Tryptophan is an important and frequently used material in the chemicals synthesis of a range of pharmaceuticals. It cannot be synthesized in the human body and thus must be obtained from food or supplements. It is a precursor of the vital neurotransmitter, serotonin, tryptophan levels in the body regulate moods and sleep [19,20].

Isonitrosoacetophenone (HINAP) (Fig. 1) is expected to behave as potential ambidentate ligands. It forms stable chelates with transition metal ions showing a variety of structural features. It can coordinate either through nitrogen or oxygen atom. While the binary complexes of HINAP with transition metal ions are known and their use in the catalysts has been reported, its uses in the formation of ternary transition metal complexes has not been reported so far.

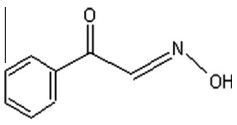

Fig. 1. Structure of isonitrosoacetophenone (HINAP).

For the present study, we report the synthesis and the characterization of ternary copper (II) complexes with amino acids and oxime. For this, we have chosen α-amino acids, abbreviated in general as HL (where H is the dissociable carboxylic proton) and isonitrosoacetophenone. The α-amino acids are known to bind to metal ion via dissociation of the acidic proton as bidentate N,O-donor forming five-membered chelate rings [14].

The synthesized complexes have been studied electrochemically. In view of the above points, we have also extended our investigations to antifungal and antibacterial properties of these ternary Cu (II) complexes.

Free radicals play an important role in the inflammatory process. They are an integral part of human metabolism [21,22]. Antioxidant compounds play an important role as a health-protecting factor. Scientific evidence suggests that antioxidants reduce the risk for chronic diseases including cancer and heart disease. Compounds with possible antioxidant properties could play crucial role against inflammation, lead to potentially effective drugs and may protect organism against free radical damage [23].

The main characteristic of an antioxidant is its ability to trap free radicals. These free radicals can initiate degenerative disease. So, antioxidant compounds defend the organisms against free radical damage and then help the human body to reduce oxidative damage [24].

The aims of our study is to examine in vitro, the capacity of the ternary complexes of oxime and amino acids to scavenge the form of RS such as 2,2-diphenyl-1-picrylhydrazyl (DPPH·) [25].

An attempt to gain a better insight on the molecular structure of the studied copper complexes, theoretical calculations using the DFT computation technique for the optimized geometries of the compounds have been used to define the electronic configuration and to explain the spectroscopic and electrochemical properties of the molecules. The final aim and the expectation of this work is to have information if these complexes may be of potential biological importance.

Experimental

Reagents and apparatus

All the chemical reagents and solvents used in the preparations were Fluka p.a. products and used without further purification.

The elemental microanalysis was carried out by the Laboratoire de Chimie de Coordination, CNRS, Toulouse (France).

Melting points were measured using a Büchi 512 digital melting point apparatus.

Conductivity measurements were carried out using 10^{-3} M solution in ethanol on a SELECTA CD 2005 apparatus employing a calibrated dip-type cell at 25 °C.

The IR spectra were recorded on Perkin Elmer FT-IR Spectrometer Spectrum-One Model, in the range 4000–400 cm^{-1}, using KBr discs.

The electronic absorption spectra in ethanol solution were recorded on a UV–Visible JASCO V 560 spectrophotometer using quartz cells, in the UV and Visible range, 1100–200 nm.

X Band EPR spectra were taken on an Elexys E500 Bruker spectrometer in frozen solution.

Cyclic voltammograms were obtained using PG210 VOLTA Lab. The working, counter and reference electrodes were, respectively, a platinum wire, a platinum foil and SCE (saturated calomel electrode). The SCE was separated from the test solution by a bridge filled with the solvent and supporting electrolyte which was tetrabutylammonium perchlorate (TBAP). The inert gas used was nitrogen. The ionic strength is 1 mol L^{-1}.

Coulometric measurements were made using a double circular platinum net as working electrode. The auxiliary and reference electrodes, the blank electrolyte solution and the inert gas were the same as in voltammetric measurements. The temperature in all the experiments was 25.0 ± 0.1 °C.

Biological studies

Microorganisms and culture conditions

The growth inhibitory activity of the chemical matter was tested against six bacteria [*Escherichia coli* (*ATCC 4157*), *Staphylococcus aureus* (*ATCC 6538*), *Streptococcus pyogenes* (*ATCC 12358*), *Proteus mirabilis* (*ATCC 49565*), *Pseudomonas aeruginosa* (*ATCC 9027*), *Bacillus subtilis* (*ATCC 9372*)] and one yeast *Candida albicans* (*ATCC 24433*). The antimicrobial and antifungal activities of the ligands and their metal complexes were determined using the agar-disc diffusion method as will be described below. Mueller–Hinton agar (MHA) and Sabouraud dextrose agar (SDA) were used to test the sensitivity of the bacteria and the yeast. The MHA and SDA, sterilized and cooled to 45–50 °C, were distributed into sterile Petri dishes [26]. The bacteria were first incubated at 37 °C for 24 h in nutrient agar, MHA and when melted poured into plastic Petri dishes. The yeast was incubated in Sabouraud dextrose agar at 25 °C for 48 h. The cultures of the bacteria and yeast were injected into the Petri dishes (9 cm) in the amount of 0.1 mL. The compounds were dissolved at a concentration of 10 mg/mL in DMSO.

Controls were performed for each bacteria strain and the yeast, where 0.1 mL of the pure solvent was inoculated into the well. The mean value obtained for three individual replicates was used to calculate the zone of growth inhibition of each sample.

Sulfamethoxazole (SMX) and Ampicillin were used as a standard reference in the case of bacteria while ketoconazole, Amphotericine B were used as a standard antifungal Ref. [27].

The results were read by measuring the diameters of the inhibition zones in millimeter.

Antioxidant study

Antioxidant properties of ternary complexes of copper (II) were determined spectrophotometrically in one test. Radical scavenging 2,2-diphenyl-1-picrylhydrazyl radical (DPPH) has a violet coloring, the intensity of which decreases in the presence of antioxidant proportionally to the ability to "sweep of" free radicals by the tested compound.

DPPH is characterized as a stable free radical due to the delocalization of the spare electron over the molecule. The delocalization gives rise to a deep violet color characterized by an absorption band at 517 nm.

When the odd electron of DPPH becomes paired off, the absorption decreases significantly.

Hence, more rapidly the absorbance decrease, the more potent is the antioxidant activity of the compound. The hydrogen atom or electron donation ability of the compound was measured from the bleaching of the purple-colored methanol solution of DPPH.

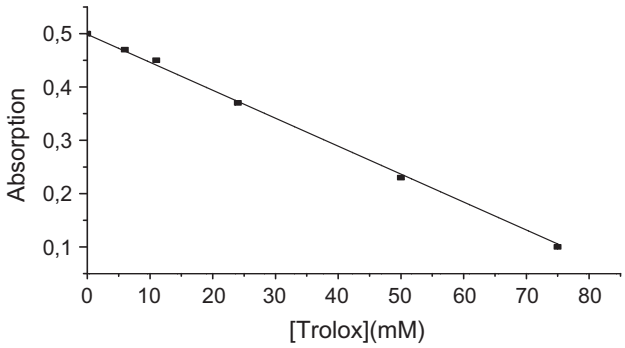

Fig. 2. Calibration curve for DPPH absorption.

The sample of complexes (0.1 mL) were mixed with 3.9 mL of methanolic solution containing DPPH radicals (6.34×10^{-5} mol/L). The mixture was shaken vigorously and left in the dark until stable absorption value was obtained. The reduction of the DPPH radical was measured by monitoring continuously the decrease of absorption at 517 nm. DPPH scavenging effect was calculated as percentage of DPPH discoloration using the equation [28]:

$$\% \text{ Scavenging effect} = [(A_{DPPH} - A_S)]/A_{DPPH}] \times 100$$

where A_S is the absorbance of the solution when the sample has been added and DPPH is the absorbance of the DPPH solution. Results are expressed in mmol trolox equivalents/L. All the tests were replicated thrice.

The following calibration curve of the absorption of DPPH was plotted, it will be used to estimate the antioxidant power of the ligands and the copper complexes which will be expressed in trolox equivalent (see Fig. 2).

Synthesis of the complexes

The mixed-ligand copper(II) complexes were prepared from copper(II) chloride, HINAP and various amino acids such as histidine, phenylalanine and tryptophan as described below.

To a green-colored ethanolic (50 mL) solution of copper (II) chloride dihydrated (17.04 mg, 5 mmol) was added an ethanolic (50 mL) solution of HINAP (745 mg, 5 mmol).

The mixture was stirred and kept in a water bath at 50 °C for 30 min, during which time the mixture turned dark green. To this was added 1:1 aqueous ethanolic (50 mL) solution of the amino acid (5 mmol) the mixture (1:1:1 M proportion) was refluxed for 4 h, when a green to brown colored solid precipitated.

The mixture was cooled and the solid was filtered, washed with ice-cold water followed by ice-cold ethanol. The complexes thus prepared were dried under vacuum.

Computational details

Quantum Chemical calculations were performed with GAUSSIAN 03 program packaged [29]. The geometry of the complexes was optimized using Density Functional Theory (DFT). All theoretical calculations were carried out at gradient corrected DFT using Becke's three parameter hybrid method and the Lee–Yang–Parr correlation functional B3LYP [30] combined with LANL2DZ basis set [31].

The studied forms of complexes were characterized as minima (no imaginary frequency) in their potential energy surface through harmonic frequency analysis and their vibration spectra were analyzed using GABEDIT software [32].

Table 1
Characteristic and analytical data of copper complexes.

Compound	Color	Yield (%)	Mp (°C)	Elemental analysis (%) found (calc.)				Conductance in ethanol (Ω^{-1} cm^2 mol^{-1})
				Cu	C	H	N	
[Cu(INAP)(Hist)(H_2O)$_2$]	Brown	68	190	15.19 (14.84)	36.98 (35.99)	3.95 (3.73)	12.29 (13.1)	2.4
[Cu(INAP)(Phen)(H_2O)$_2$]	Green	54	163	14.25 (14.47)	54.32 (54.89)	4.26 (3.72)	7.45 (7.44)	3.4
[Cu(INAP)(Tryp)(H_2O)$_2$]	Green	50	210	13.85 (13.20)	50.42 (51.13)	4.59 (4.77)	9.19 (9.55)	5

Mp: melting point.

Results and discussion

Analytical data of metal complexes

The mixed complexes of copper (II) with isonitrosoacetophenone and amino acids were synthesized in 1:1:1 M proportion.

Where INAP and HL represent deprotonated isonitrosoacetopenone and amino acids, respectively. All the complexes are brown to dark green in color and are in general, non-hygroscopic solids, insoluble in water but soluble in common organic solvents such as ethanol, methanol, DMSO, and DMF. The non-electrolyte nature of the complexes was confirmed by the low molar conductance values measured at 25 °C in 10^{-3} M ethanol solution [33]. The physical properties and analytical data of the complexes are summarized in Table 1. The copper complexes were obtained as powders and attempts to obtain single crystal suitable for X-ray determination were unsuccessful.

Infrared spectra

The most important assignments IR bands are shown in Table 2. The ligands coordination sites which are involved in bonding with the metal ions have been determined by careful comparison of the infrared absorption spectra of the complexes with those of the parent ligands. The vibrational assignments were carried out with support DFT calculations using the B3LYP method with LANN2DZ basis set. The experimental and theoretical FT-IR spectra of Cu-INAP-Phen are given in Fig. 3, while the corresponding frequencies along with the assignments are tabulated in Table 2.

The IR spectra of amino acids exhibited significant features in $\nu(NH_3^+)$ and ν(COO—) regions. The stretching vibration $\nu(NH_3^+)$ is observed in the range 3015–3067 cm^{-1}. The corresponding theoretical values of this vibration are in the region 2982–3100 cm^{-1}. The $\delta(NH_3^+)$ band, which is a characteristic for the zwitter ion, disappeared in the spectra of the complexes. The $\nu(NH_3^+)$ stretching vibration shifts to the lower regions in the spectra of the complexes. This may indicates that the NH_2 group must be involved in coordination. A broad band of ν(OH) group in the IR spectra of the oxime is observed at 3290 cm^{-1}. This band is absent in the spectra of copper complexes, suggesting the deprotonation of the HINAP.

The bands with medium intensity observed in the range 3441–3495 cm^{-1} of the copper complexes are attributed to ν(OH) of coordinated water. The bands at 810–861 and 610–613 cm^{-1} are assigned to $\rho_r(H_2O)$ and $\rho_w(H_2O)$ [34]. Calculated value of this absorption band is in the range 3431–3478 cm^{-1}. The strong absorption band at 1677 cm^{-1} is assigned to the coupled vibration of C=O stretching of the oxime [35]. In the copper complexes, this vibration is shifted to the lower regions by 11–55 cm^{-1} indicating the formation of a bond between the metal ion and the C=O group [36], while the theoretical values are established in the range 1644–1664 cm^{-1} as calculated by B3LYP method. The medium band observed around 1593 cm^{-1} in the oxime is due to the vibration of C=N stretching vibration. The red shift of this band appears in the region of 1516–1546 cm^{-1} after complexation [37]. The calculated vibrational frequencies were found in the range 1499–1546 cm^{-1}. This indicates that the oxime acts as a bidentate anion and that the coordination is both through the nitrogen donor atom of the azomethine group and the oxygen of the carbonyl group. The N → O stretching vibration appears in the range 1213–1230 cm^{-1} in the Cu(II) complexes [36,38,39]. The computed wavenumber for this vibration is in the region 1221–1259 cm^{-1}.

Complementary evidence of the bonding is also shown by the fact that new bands of medium intensity in the IR spectra of the complexes appear at 510–523 cm^{-1} and 483–433 cm^{-1} assigned to ν(M—O) and ν(M—N) stretching vibrations. The calculated ν(M—O) and ν(M—N) modes were found in the region 520–537 cm^{-1} and 427–453 cm^{-1}, respectively. In general, the absorption frequencies obtained from experiment and theory are in good agreement.

Electronic spectra

The electronic absorption spectra of Cu(II) chelates recorded in ethanol solution show three prominent bands or shoulders in the range 26,315–38,461 cm^{-1} which are due to the intraligand transitions ($n \rightarrow \pi^*$ and $\pi \rightarrow \pi^*$) [40].

Cu (II) mixed complexes reveal a large band in the 12,578–14,326 cm^{-1} region and one shoulder in the range 19,047–21,052 cm^{-1}. The large band is assigned to $^2B_{1g} \rightarrow {}^2B_{2g}$ and the shoulder is attributed to the transition $^2B_{1g} \rightarrow {}^2E_g$ assuming pseudo octahedral stereochemistry for all Cu (II) complexes [41].

The magnetic moments are equal to 2.06, 1.93 and 1.66 B.M. respectively for [Cu(INAP)(Hist)(H_2O)$_2$], [Cu(INAP)(Phen)(H_2O)$_2$] and [Cu(INAP)(Tryp)(H_2O)$_2$] which are close to the spin only value for the unpaired electron. Effective moments were calculated from room temperature magnetic susceptibilities and using diamagnetic corrections from the literature [42,43]. These values are within the ranges reported for a distorted octahedral substituted six-coordinate Cu (II) with two dianionic ligands and two water molecules [43]. The results of Table 3 show that tryptophan causes a higher crystal field than phenylalanine and histidine. The order of crystal field is Hist < Phen < Tryp.

The oscillator strengths for the observed bands in the UV–Vis spectra are approximately evaluated, assuming bands as Gaussian curves, using the following expression:

$$f_{obs} = 4.610^{-9} \cdot \varepsilon_{max} \cdot \Delta\overline{\upsilon}_{1/2} \ (cm^{-1})$$

ε_{max} is the molar extinction coefficient, $\overline{\upsilon}$ is the wavenumber and $\Delta\overline{\upsilon}_{1/2}$ is the bandwidth at half height.

Theoretical wavelengths (λ) and oscillators' strengths of the electronic transitions were calculated by the TDDFT method at the UB3LYP/LanL2DZ level.

The oscillators' strengths of the two observed transitions in copper (II) complexes, are very small (< 0.01). It is characteristic of spin allowed and symmetry forbidden d–d transitions.

We can also notice that there is a reasonable agreement between the experimental and calculated values of wavelengths and oscillator strengths. The variation of these parameters is the same for the three complexes.

The experimental and calculated results of UV–Vis spectral data were compared in Table 3.

ESR spectroscopy

ESR spectra of Cu (II) complexes were recorded on X band at a frequency range of 9.4–9.5 GHz at 173 K temperature in frozen DMSO glass. The ESR spectra of the complexes are of an anisotropic type for mononuclear species with axial symmetry. The $g_{//}$ and $g_{\perp}$ parameters are summarized in Table 4. The trend $g_{//} < g_{\perp} < g_e$ (2.00023) observed in these complexes shows that the unpaired electron is in the $d_{x^2-y^2}$ orbital of copper(II) [44]. This suggest distortion in the Cu (II) complexes from O_h symmetry to D_{4h} symmetry. They also show that $g_{//} = 2.32–2.39$ which is in conformity with the presence of mixed copper–nitrogen and copper–oxygen bonds in these chelates [45].

The ESR spectra of the copper complexes exhibit a set of four hyperfine lines corresponding to the interaction of the electron of the Cu ion with its nuclear spin $I_{cu} = 3/2$. The values of $g_{//}$ and $g_{\perp}$ are characteristic of an N_2O_4 arrangement [46]. The quotient $g_{//}/A_{//}$ measures the distortion from planarity [47,48]. The distortion from the plane increases with increasing $g_{//}$ values and decreasing $A_{//}$ values. The lowering of $A_{//}$ values of the complexes reflects a lower symmetry for the complexes.

Indeed, according to DFT calculations this could be explained by the increase of the dihedral angles (N2—Cu1—O5—C29) and (N3—Cu1—N2—C13) on going from histidine to tryptophan (see Table 5).

These dihedral angles are formed by two metal–ligand bonds which are significant of the deformation of the copper coordination sphere. The larger the variation of dihedral angle is, the greater distortion will be.

In the complexes the parameter $g_{//}$ is well resolved unlike the $g_{\perp}$. The g_{av} value for the complexes is greater than 2 indicating covalent nature of the metal–ligand bond. The value of $g_{//}$ decreases on going from histidine to tryptophan. So, to have a better understanding of the nature of the metal–ligand bonding in these complexes, various bonding parameters have been evaluated from the low temperature ESR spectra. The in-plane σ bonding (α^2) and of the in-plane π bonding (β^2) were estimated for each monomeric species by using the following expressions, where λ_0 represents the one electron spin–orbit coupling constant for the free ion, equal to $-828\ cm^{-1}$.

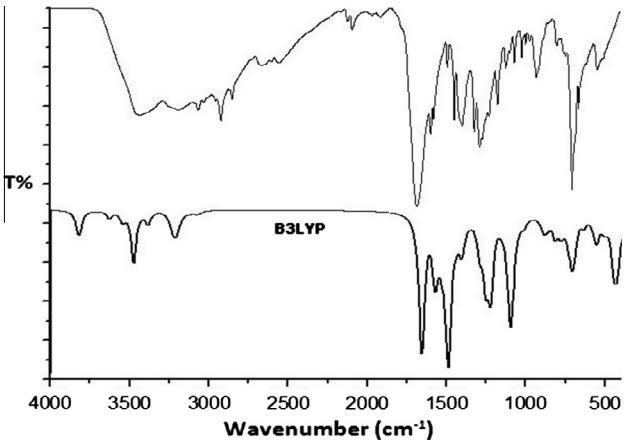

Fig. 3. Experimental and theoretical FT-IR spectra of Cu-INAP-Phen.

Table 3
Wavelengths (λ), oscillators strengths (f) and d–d electronic transitions of the studied complexes.

λ_{exp}[a] (nm)	f_{exp}[b]	λ_{th}[c] (nm)	f_{th}[d]	d–d Electronic transitions
[Cu(INAP)(Hist)(H2O)2]				
795	0.0034	790	0.0058	b_{2g} (d_{xy}) → b_{1g} (d_{x2-y2})
525	0.0032	568	0.0037	e_g (d_{xz}, d_{yz}) → b_{1g} (d_{x2-y2})
[Cu(INAP)(Phen)(H2O)2]				
740	0.0009	784	0.0022	b_{2g} (d_{xy}) → b_{1g} (d_{x2-y2})
510	0.0014	571	0.0039	e_g (d_{xz}, d_{yz}) → b_{1g} (d_{x2-y2})
[Cu(INAP)(Tryp)(H2O)2]				
698	0.0017	739	0.0030	b_{2g} (d_{xy}) → b_{1g} (d_{x2-y2})
475	0.0035	569	0.0040	e_g (d_{xz}, d_{yz}) → b_{1g} (d_{x2-y2})

[a] λ_{exp} = experimental wavelength.
[b] f_{exp} = experimental oscillator strength.
[c] λ_{th} = theoretical wavelength.
[d] f_{th} = theoretical oscillator strength.

$$\alpha^2 = \frac{A_{//}}{0.036} + (g_{//} - 2.0023) + \frac{3}{7}(g_{\perp} - 2.0023) + 0.04$$

$$\beta^2 = -(g_{//} - 2.0023)\frac{\Delta E_{xy}}{8\lambda_0\alpha}$$

The theoretical ESR parameters are evaluated by DFT calculations for comparison with the experimental ones (see Table 4).

The values of bonding parameters evaluated from ESR spectra are in reasonable agreement with those calculated by DFT. We also notice that the theoretical values of $g_{//}$ and $g_{\perp}$ decrease in the same order than the experimental ones.

By examining the trend of the α^2 and the β^2 values obtained, it can be seen that the covalent character in the mixed copper (II)

Table 2
Relevant IR data (cm^{-1}) of the ligands and the complexes..

Compound	ν(O—H)	$\nu(NH_3^+)_{as}$	ν(C=O)	$\nu(COO—)_{as}$	$\nu(COO—)_s$	ν(C=N)	ν(N—O)	ν(M—O)	ν(M—N)
HINAP	3291s	–	1677s	–	–	1593 m	1238s	–	–
Histidine	3439m	3015m	–	1587s	1414m	–	–	–	–
Phenylalanine	3465s	3067m	–	1560s	1409m	–	–	–	–
Tryptophan	3404s	3039m	–	1591s	1414m	–	–	–	–
[Cu(INAP)(Hist)(H2O)2]	3441s	2924s	1658s	1596m	1387m	1516m	1230m	523w	461w
	(3431)	(2936)	(1664)			(1546)	(1259)	(537)	(428)
[Cu(INAP)(Phen)(H2O)2]	3445s	2913s	1666s	1595m	1383m	1546s	1227m	514w	486w
	(3461)	(2949)	(1661)			(1533)	(1226)	(520)	(427)
[Cu(INAP)(Tryp)(H2O)2]	3495s	2921s	1622s	1594s	1379m	1519m	1213s	510w	433w
	(3478)	(2952)	(1644)			(1499)	(1221)	(525)	(453)

Found: experimental (calc.): calculated by DFT s = strong, m = medium, w = weak.

Table 4
ESR parameters of Cu (II) complexes.

Complex	$g_{//}$	$g_{\perp}$	$A_{//}$ (10^{-4})	$g_{//}/A_{//}$	α^2	β^2
Cu-INAP-Hist	2.392 (2.46)	2.082 (2.21)	118 (87)	202 (282)	0.787 (0.780)	0.830 (0.729)
Cu-INAP-Phen	2.345 (2.13)	2.075 (1.92)	120 (89)	195 (239)	0.747 (0.745)	0.813 (0.660)
Cu-INAP-Tryp	2.325 (1.99)	2.066 (1.90)	128 (104)	181 (191)	0.735 (0.749)	0.811 (0.538)

Found: experimental (calc.): calculated by DFT.

Table 5
Calculated bond distances (Å), angles (°) and dihedral angles (°) of the copper (II) complexes computed using B3LYP/LANL2DZ.

Parameters	Complexes		
	Cu-INAP-Hist	Cu-INAP-Phen	Cu-INAP-Tryp
Bond length (Å)			
Cu1—N2	2.019	2.020	2.030
Cu1—N3	2.048	2.013	2.012
Cu1—O4	1.975	1.995	2.006
Cu1—O5	2.282	2.048	2.054
Cu1—O6(H_2O)	2.114	2.214	2.426
Cu1—O7(H_2O)	2.353	2.275	2.498
Bond angles (°)			
N2—Cu1—N3	99.96	95.38	95.82
N2—Cu1—O4	83.00	81.98	83.25
N2—Cu1—O5	172.66	161.19	171.52
N3—Cu1—O5	90.91	80.51	80.52
N3—Cu1—O4	173.64	175.44	176.39
O4—Cu1—O5	96.62	100.79	99.93
O4—Cu1—O6	84.48	61.55	71.59
O5—Cu1—O6	112.04	100.25	90.71
O7—Cu1—N2	95.70	108.12	104.95
O7—Cu1—N3	94.36	106.87	109.86
O7—Cu1—O6	152.78	168.90	175.16
Dihedral angles (°)			
N2—Cu1—O5—C29	−157.99	−79.29	−64.42
N3—Cu1—N2—C13	144.59	151.46	163.08
H8—O6—Cu1—O4	−122.58	−136.66	−148.69
H11—O7—Cu1—N2	173.53	136.21	159.34
O14—C12—O4—Cu1	−179.62	−178.6	−177.34
C29—O5—Cu1—O4	−74.62	−176.13	−175.86
C41—C29—O5—Cu1	−14.98	−0.52	−0.32

complexes with the amino acids should increase in the order of hist < phen < tryp. This order satisfactorily correlates with electron density at the nitrogen donor atom which shows the same trend.

Geometry optimization

Selected bond distances, angles and dihedral angles for the three complexes are listed in Table 5. On the basis of the results obtained by spectroscopic investigations (FTIR, UV–Vis and ESR) of these complexes, we suggest that the ligands are coordinated in a deprotonated form, through oxygen and nitrogen atoms leading to neutral complexes.

Indeed, according to the DFT study, the Cu(II) adopts a distorted octahedral geometry, where INAP acts as a bidentate ligand through both the imine nitrogen and carbonyl oxygen [Cu1—N3 = 2.048–2.012 Å and Cu1—O5 = 2.282–2.048 Å]. The amino acid also acts as a bidentate ligand through carboxylate oxygen and nitrogen of NH_2 [Cu1—O4 = 1.975–2.006 Å and Cu—N2 = 2.019–2.030 Å]. The ligands give a square planar arrangement of N_2O_2 donor groups around the copper ion. The other axial sites being occupied by water molecules.

In all complexes, the Cu—O4 bond length is shorter than the Cu1—O5 bond length indicating that the coordination ability of carboxylate oxygen is stronger than that of carbonyl oxygen of INAP. It is also noticed from the DFT data, the distance of Cu—N2 to be shorter than that of Cu—N3. Hence, the coordination ability of nitrogen atom of C=N is weaker than that of N atom of NH_2 [49]. Two aqua ($O6H_2$ and $O7H_2$) molecules are lying in the molecular plane in *trans* position with a bond angle of (152.78–175.16°). The O7=Cu1=O6 angles deviate from linearity (180°) indicating a distortion in the basal plane. The bond lengths of Cu1=O6 and Cu1=O7 increase on going from histidine to tryptophan. Axial elongation can easily be explained in terms of the Jahn–Teller distortion observed in most octahedral Cu(II) [50]. The values of Mulliken charges show the cationic property of Cu while the atoms of the ligands surrounding the metal show an anionic property (Table 6).

The charge of Cu decreases from Cu-INAP-Tryp to Cu-INAP-Hist. Copper complexes with histidine has the highest charge of Mulliken compared with the two other forms, this can be explain by the presence of three atoms of nitrogen in the amino acid (see Table 6).

A view of the optimized structure of Cu-INAP-Hist complex and its atom numbering are shown in Fig. 4. Indeed, it was found that the *trans*-copper(II) complexes are more stable energetically than *cis*-copper(II) complexes. The difference of energy ΔE between *cis* and *trans* is = 12.8 kcal/mol for [Cu(INAP)(Hist)(H_2O)$_2$], 41.16 kcal/mol for [Cu(INAP)(Phen)(H_2O)$_2$] and 141 kcal/mol for [Cu(INAP)(Tryp)(H_2O)$_2$] [51]. Values of the HOMO–LUMO energy separation, the gap, estimated for the copper complexes are equal to 1.91 eV, 2.56 eV and 2.67 eV respectively for [Cu(INAP)(Hist)(H_2O)$_2$], [Cu(INAP)(Phen)(H_2O)$_2$] and [Cu(INAP)(Tryp)(H_2O)$_2$]. Thus, the greater the energy gap is, the higher the stability is. So, [Cu(INAP)(Tryp)(H_2O)$_2$] is the more stable complex because it possesses the highest energy gap. According to what has been reported in the literature, binary copper complex with the tryptophan is the most stable one according to the value of formation constant compared to copper complexes with histidine and with phenylalanine [52]. The latter increases in the order Hist < Phen < Tryp. Thus, we can predict that the stability of the ternary copper complexes increases in the same order.

Table 6
Dipole moments and Mulliken charges.

Parameters	Complexes		
	Cu-INAP-Hist	Cu-INAP-Phen	Cu-INAP-Tryp
Dipole moment (Db)	8.55	6.36	5.28
Mulliken charges	Cu: 0.547 N2: −0.688 N3: −0.043 O4: −0.420 O5: −0.375 O6: −0.759 O7: −0.816	Cu: 0.478 N2: −0.693 N3: −0.072 O4: −0.494 O5: −0.398 O6: −0.765 O7: −0.699	Cu: 0.429 N2: −0.702 N3: −0.066 O4: −0.496 O5: −0.399 O6: −0.721 O7: −0.707

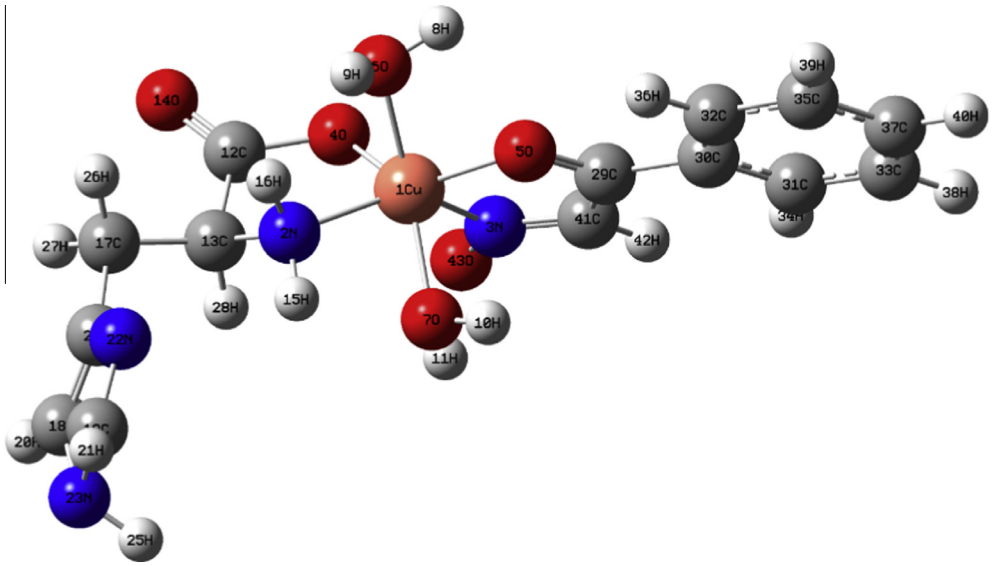

Fig. 4. The optimized structure of [Cu(INAP)(Hist)(H_2O)$_2$].

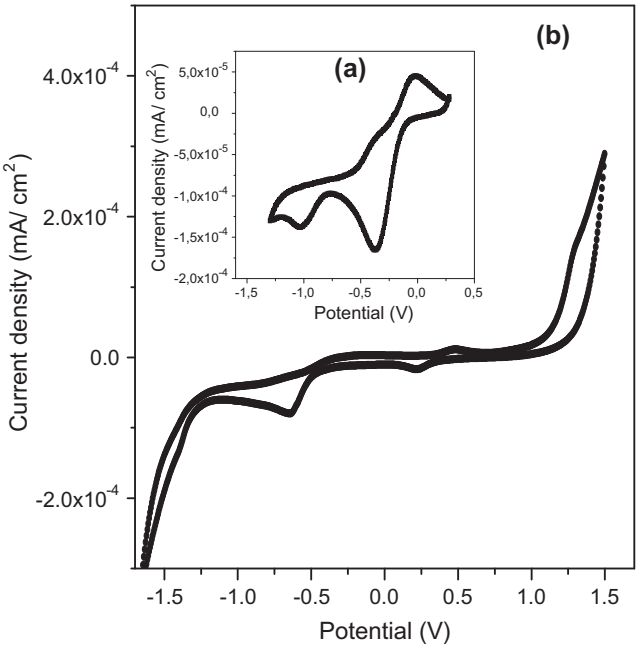

Fig. 5. Cyclic voltammograms of (a) $CuCl_2$ (b) Cu-INAP-Tryp complex in DMSO (0.1 M TBAP); scan rate = 10 mV/s, (inset: behavior of $CuCl_2$).

Electrochemistry

The electrochemical profiles of the ligands of amino acids and isonitrosoacetophenone and their complexes were studied in DMSO by cyclic voltammetry from +1.5 to −1.5 V (vs. SCE). The electrochemical experiments were done at room temperature (25 °C).

Coulometric analysis indicates that each of the processes involves a one-electron transfer.

Cyclic voltammogram of $CuCl_2$ shows two irreversible reduction processes at −0.32 V assigned to the couple CuII/CuI and −0.96 V attributed to CuI/Cu and a single anodic peak at +0.64 V without any associated cathodic response. The anodic wave at 0.92 V is observed in all the cyclic voltammograms of the ligands, it can be attributed to an irreversible oxidation process (Fig. 5).

Table 7
Electrochemical data for the reduction of the ligands, $CuCl_2$ and the Cu(II) complexes[a] in 0.1 M TBAP in DMSO.

Compounds	Epc (V)	Epa (V)	ΔE (mV)
HINAP	−0.524	–	–
	−0.756	−0.554	202
Histidine	−0.466	–	–
Phenylalanine	−0.532	–	–
Tryptophan	−0.549	–	–
$CuCl_2$	−0.320	0.140	460
	−0.960	−0.380	560
[Cu(INAP)(Hist)(H_2O)$_2$]	0.365	0.425	60
	−0.482	−0.299	183
[Cu(INAP)(Phen)(H_2O)$_2$]	0.360	0.414	54
	−0.540	−0.343	197
[Cu(INAP)(Tryp)(H_2O)$_2$]	0.227	0.417	19
	−0.647	−0.360	287

[a] Solute concentration = 10^{-3} M, scan rate = 10 mV/s; Epc and Epa are the cathodic and the anodic peak potentials respectively; ΔE = Epa − Epc.

The electrochemical data on the reduction of the complexes at a sweep rate of 10 mV s^{-1} are given in Table 7.

The reduction voltammograms of the histidine, phenylalanine and tryptophan display one cathodic peak located at −0.466, −0.542, −0.549 respectively. The cyclic voltammogram of isonitrosoacetophenone (HINAP) shows reduction signals at the cathodic potential peak Epc_1 = −0.524 V and Epc_2 = −0.756 V, attributed to the insaturation of the ligand.

By comparing the cyclic voltammograms of complexes to those of the ligands and that of the $CuCl_2$, $6H_2O$ taken as reference, the reduction process should correspond to Cu (II/I). The metal centered reduction for all the copper complexes shows an irreversible electron transfer [53]. Further, the reduction waves given by the voltammograms with the cathodic scan are of medium intensity.

The more negative cathodic potentials for the Cu (II)/Cu(I) couple of complexes are seen in the order of Tryptophan < Phenylalanine < Histidine, that correlates with the steric and electronic effects of the R group of the amino acid. Finally, an increase of the electron density on the copper increases the

Table 8
Results of antibacterial activity screening of ligands and copper complexes.[a]

Compound	Inhibition zone diameter (mm)						
	S. aureus	*S. pyogenes*	*B. subtillis*	*E. coli*	*P. aeruginosa*	*P. mirabilis*	*C. albicans*
HINAP	14	13	11	12	–	13	–
Histidine	10	–	–	14	–	11	–
Phenylalanine	16	–	–	20	11	13	–
Tryptophan	19	–	–	18	12	14	–
Cu-INAP-Hist	12	11	–	12	12	–	17
Cu-INAP-Phen	14	14	13	12	14	–	18
Cu-INAP-Tryp	15	17	18	13	16	24	26
Sulfamethoxazol	28	Nt	29	36	–	Nt	–
Ampicillin	11	12	Nt	08	Nt	–	–
Ketoconazol	–	–	–	–	–	–	38
Amphotericin B	–	–	–	–	–	–	29

Nt not tested, (–) no activity.
[a] Where INAP represent isonitrosoacetophenone and Hist, Phen and Tryp represent deprotonated histidine, phenylalanine and tryptophan, respectively.

difficulty of reducing the metal center and stabilize the high oxidation state for the metal ion [54,55]. We also note that the power of ligand field increases on going from histidine to phenylalanine to tryptophan.

This results may be correlated with the HOMO and LUMO energies. The study of frontier orbital and the geometrical parameters show that for the complex Cu-INAP-Tryp, unlike the other complexes, the LUMO is mainly located on the INAP and moves towards on the metal (see Fig. 5). This makes the access of foreign electron to metal orbitals, difficult. This proves that the structure of the complex depending on the nature of the ligand surrounding the center metal, affects the electrochemical behavior of complex and consequently the reduction and oxidizing of the metal center. The [Cu(INAP)(Tryp)$(H_2O)_2$] owns the lowest reduction potential which is in a good agreement with the highest value of the LUMO. LUMO of Cu-INAP-Hist has the lowest energy value, so it is the most stable one. It means that the complex Cu-INAP-Hist will be more easily reduced as it has the larger electron affinity. We could also relate the reduction potential to HOMO since it is partially filled in the case of copper which has d^9 electronic configuration, so the HOMO could accept one electron. Reduction potential Epc shifts towards more negatives values on going from histidine to tryptophan.

The HOMO measures the electron donating ability to donate an electron, LUMO as an electron acceptor represent the ability to obtain an electron.

Thus, the larger the E_{HOMO} is, the greater the electron donating capacity will be, and the smaller the E_{LUMO} is, the smaller the resistance to accept electrons will be [51].

Antibacterial activity

The mixed copper (II) complexes were investigated for their microbial activity against pathogenic bacterial and fungal species using disc diffusion method. The results of the bacterial screening of the synthesized compounds are recorded in Table 8. No growth inhibition was observed for DMSO and copper chloride salt.

The primary ligand, HINAP, and the amino acids have moderate activity with *S. aureus, P. mirabilis* and *E. coli* and are more active in comparison with *S. pyogenes* and *B. subtilis.* Therefore, copper(II) complexes exhibit a good activity with *S. pyogenes* and *B. subtilis*, among Gram-positive and Gram-negative bacteria studied. Cu-INAP-Tryp showed more activity than Cu-INAP-Hist and Cu-INAP-Phen against in all tested microorganisms. It is clearly observed that the copper complexes are very active against the fungus *C. albicans*.

The mixed complexes of tryptophan exhibit the most higher activity than those of histidine and even those with phenylalanine.

This would suggest that chelation could facilitate the ability of the complex to cross a cell membrane and can be explained on the basis of Tweedy's chelation theory [56].

On chelation the polarity of the metal ion will be reduced because of the partial sharing of the positive charge of the metal with the donor groups present in the ligand. Further, it increases the delocalization of π-electron over the whole chelating space [57,58].

This increases the lipophilic character of the metal chelates and favors its permeation through the lipoid layer of the bacterial membranes. We conclude that complexation increases the antimicrobial activity. This result is correlated by the DFT calculations. The HOMO–LUMO energy separation can be used to predict reactivity of the studied compounds. The theoretical analysis of the energy gap (ΔE) of these compounds showed direct correlation with their antimicrobial activity since the latter increases along with the increase of the energy gap.

The dipole moment in a molecule, which results from non-uniform distribution of charges on the various atoms in a molecule, is another electronic parameter (see Table 6). Thus, the high values of dipole moment of complexes decrease clearly the antimicrobial activity. In our studied complexes the copper complex with the tryptophan possesses the higher antimicrobial activity since it has the lowest dipole moment [51].

Table 9
Results of antioxidant activity of ligands, copper (II) and complexes.

Compounds	Trolox eq.	AA%
HINAP	129.62	16
Histidine	130.6	19
Phenylalanine	132.65	22.4
Tryptophan	136.7	23
$CuCl_2{\cdot}6H_2O$	105	16.8
Cu-INAP-His	70	19.35
Cu-INAP-Phe	130	21
Cu-INAP-Tryp	182	24.5
Chlorogenic acid	51	17

AA%: antioxidant activity (%), trolox eq.: trolox equivalent.

Antioxidant activity

The antioxidant activity of Cu(II) complexes was measured in terms of their hydrogen donating or radical scavenging ability by UV–Vis spectrophotometer using the stable 2,2-diphenyl-1-picrylhydrazyl radical (DPPH) (Table 9).

DPPH radicals are stable free radicals and in the presence of molecules capable of donating H atoms, its radical character is neutralized. This is visually noticeable as the color changes from purple to yellow. When complexes as antioxidant donate protons to this radical, the initial absorbance of DPPH solution decreases.

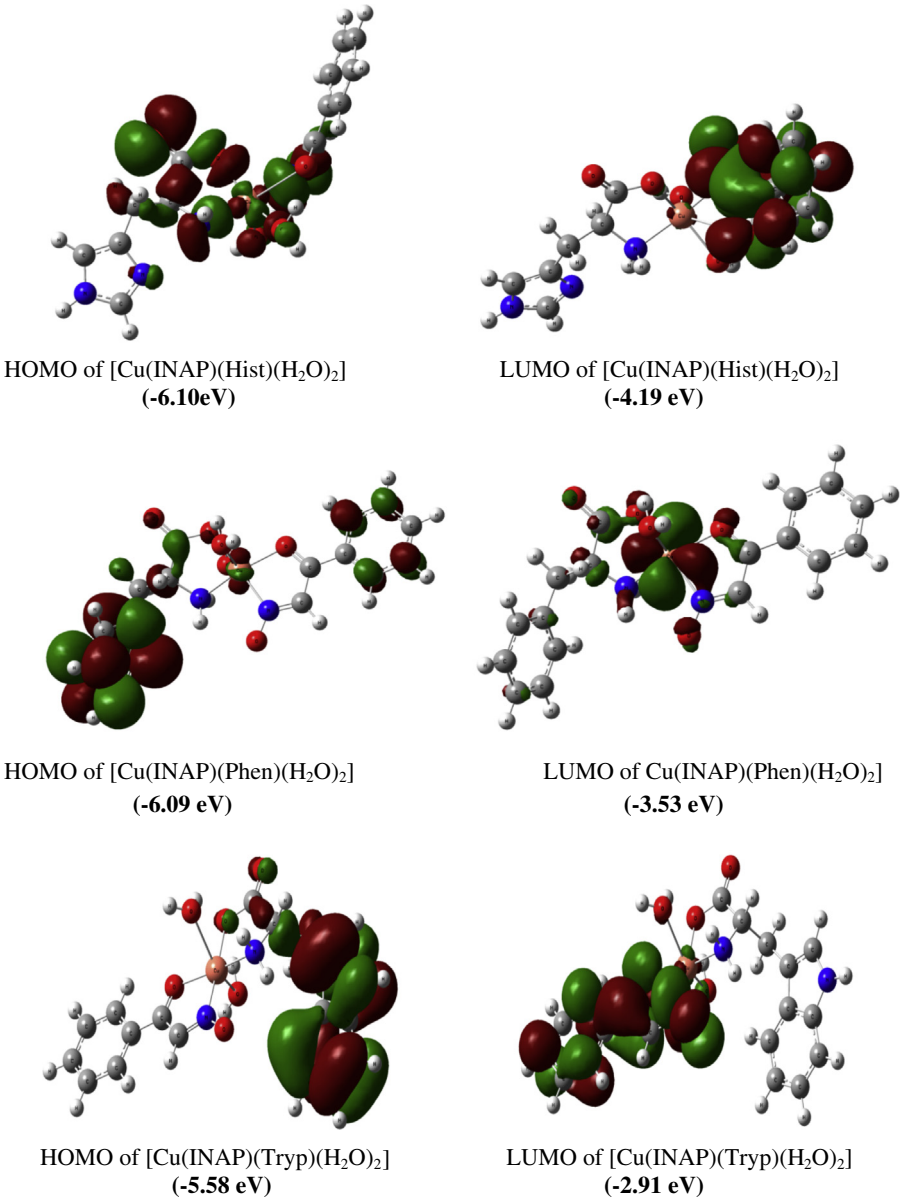

Fig. 6. Frontier molecular orbitals, HOMO and LUMO of the studied complexes.

All the Cu (II) complexes are less active than the free ligands against DPPH. Nevertheless, the antioxidant activity increases on going from histidine to tryptophan. The complex with tryptophan shows the higher antioxidant activity, this can be explain on the basis of the indole, the aromatic heterocycle that terminates the tryptophan side chain, which is both electron rich and posses an H-bond donor [59,60]. This results are correlated with DFT calculations of the HOMO and the LUMO.

For the Cu-INAP-Tryp the HOMO is localized on the tryptophan whereas the LUMO density covers completely the oxygen atoms in particular that bonded to the atom of nitrogen (N3) and the phenyl ring of INAP (Fig. 6). Hence copper complex with tryptophan is more efficient donator compound than Cu-INAP-His and Cu-INAP-Phe.

Conclusion

Cu(II) complexes with amino acids and isonitrosoacetophenone have been prepared and characterized with various spectroscopic techniques. The ternary complexes isolated are monomeric and non-electrolytes. The IR study reveals that the ligands behave as a bidentate ON donor. The electronic absorption spectra show that the ligand field is decreasing from Cu-INAP-Tryp complex to the Cu-INAP-Hist complex. This can be explained by the presence of the indole group which is both electron rich aromatic compound and possesses and H-bond donor. The electron donor effect of indole group is greater than that of imidazole one of histidine.

The DFT calculations established the optimized structure and revealed that the *trans*-copper (II) complexes are more stable energetically than *cis*-copper(II). In order to study vibrational and ESR spectroscopy, electrochemical behavior and biological activities of the copper(II) complex, the theoretical calculations were successfully performed by using DFT with the B3LYP/LANL2DZ level. The calculated data were in good agreement with the observed ones.

The ESR spectral data of copper complexes indicate that the complexes have an axial symmetry. The electrochemical behavior shows that the potential redox shift towards more negative values on going from histidine to tryptophan.

The biological activities reveal that the copper complexes have a moderate antibacterial activity but an important antifungal activity.

The antioxidant activity is moderate for all copper complexes, therefore the Cu-INAP-Tryp complex shows the better antioxidant activity because of the facility of tryptophan to donate electrons in order to reduce free radicals.

Acknowledgements

The authors are thankful to the Doctor Christelle HUREAU (CNRS, Laboratory of Coordination Chemistry, Toulouse, France) for the microanalysis, magnetic measurements and ESR analysis.

We also gratefully acknowledge Ouassila NASSI (Microbiological Laboratory of University of El Khemis, Algeria) for assistance with biological activities.

References

[1] A. Presta, M.J. Stillman, J. Inorg. Biochem. 66 (1997) 231–240.
[2] A.Y. Louie, T.J. Meade, Chem. Rev. 99 (1999) 2711–2734.
[3] Z. Balcarova, J. Kasparakova, A. Zakovska, O. Novakova, M.F. Sivo, G. Natile, V. Brabeck, Mol. Pharmacol. 53 (1998) 846–855.
[4] R.L. LaFemina, Christine L. Schneider, Helen L. Robbins, Pia L. Callahan, Kathleen Legrow, Elizabeth Roth, William A. Schleif, Emilio A. Emini, J. Virol. 66 (1992) 7414–7419.
[5] P.S. Moore, C.J. Jones, N. Mahmood, I.G. Evans, M. Goff, R. Cooper, A.J. Hay, Biochem. J. 307 (1995) 129–134.
[6] R.N. Patel, N. Singh, K. Shukla, U.K. Chauhan, S. Chakraborty, J. Niclos-Gutierrez, A. Castineiras, J. Inorg. Biochem. 98 (2004) 231–323.
[7] A.H. Fairlamb, G.B. Henderson, A. Cerami, Proc. Natl. Acad. Sci. A 86 (1989) 2607–2611.
[8] O. Rixe, W. Ortuzar, M. Alvarez, R. Parker, E. Reed, K. Paull, T. Fojo, Biochem. Pharmacol. 52 (1996) 1855–1865.
[9] R. Bakhtiar, E.I. Ochiai, Gen. Pharmacol. 32 (1999) 525–540.
[10] A. McNutt, S. Haq, R. Raval, Surf. Sci. 531 (2003) 131–144.
[11] B.B. Aggarwal, D. Danda, S. Gupta, P. Gehlot, Biochem. Pharmacol. 78 (2009) 1083–1094.
[12] C. Marzano, M. Pellei, F. Tisato, C. Santini, Anticancer Agents Med. Chem. 9 (2009) 185–211.
[13] M. Grazul, E. Budzisz, Coord. Chem. Rev. 253 (2009) 2588–2598.
[14] L.H. Abdel-Rahman, L.P. Battaglia, Polyhedron 15 (1996) 327–334.
[15] A.J. Meijer, P.F. Dubbelhuis, Biochem. Biophys. Res. Commun. 313 (2004) 397–403.
[16] S.R. de Antrade leite, M.A. Couto dos Santos, C.R. Carubelli, A.M. Galindo Massabni, Spectrochim. Acta Part A 55 (1999) 1185–1191.
[17] J.A. Cowan, Inorganic Biochemistry, An Introduction, VCH, New York, 1993.
[18] Ö. Altun, S. Bilcen, Spectrochim. Acta Part A 75 (2010) 789–793.
[19] X. Zhang, H. Yun, M. Ding, J. Chromatogr. B 877 (2009) 1678–1682.
[20] J.D. Schaechter, R.J. Wurtman, Brain Res. 532 (1990) 203–210.
[21] R. Francik, G. Kazek, M. Cegla, M. Stepniewski, Acta Pol. Pharm. 68 (2011) 185–189.
[22] K. Marxen, K.H. Vanselow, S. Lippemeier, Sensors 7 (2007) 2080–2095.
[23] G.J. Brewer, Curr. Opin. Chem. Biol. 7 (2003) 207–212.
[24] J.H. Yang, H.C. Lin, J.L. Mau, Food Chem. 77 (2002) 229–235.
[25] A.L. Dawidowicz, D. Wianowska, M. Olszowy, Food Chem. 131 (2012) 1037–1043.
[26] D. Mitic, M. Milenkovic, S. Milosavljevic, D. Godevac, Eur. J. Med. Chem. 44 (2008) 1537–1544.
[27] M. Shebl, Saied M.E. Khalil, F.S. Al-Gohani, J. Mol. Struct. 980 (2010) 78–87.
[28] C. Campos, R. Guzman, E. Lopez-Fernandez, A. Casado, Anal. Biochem. 392 (2009) 37–44.
[29] Y. Zhao, D.G. Truhlar, Theor. Chem. Acc. 120 (2008) 215–241.
[30] P.J. Hay, W.R. Wadt, J. Chem. Phys. 82 (1985) 270.
[31] M.J. Frisch, G.W. Trucks, H.B. Schlegel, G.E. Scuseria, M.A. Robb, J.R. Cheeseman, J.A. Montgomery, Jr., T. Vreven, K.N. Kudin, J.C. Burant, J.M. Millam, S.S. Iyengar, J. Tomasi, V. Barone, B., Mennucci, M. Cossi, G. Scalmani, N. Rega, G.A. Petersson, H. Nakatsuji, M. Hada, M. Ehara, K. Toyota, R. Fukuda, J. Hasegawa, M. Ishida, T. Nakajima, Y. Honda, O. Kitao, H. Nakai, M. Klene, X. Li, J.E. Knox, H.P. Hratchian, J.B. Cross, C. Adamo, J. Jaramillo, R. Gomperts, R.E. Ratmann, O. Yazyev, A.J. Austin, R. Cammi, C. Pomelli, J.W. Ochterski, P.Y. Ayala, K. Morokuma, G.A. Voth, P. Salvador, J.J. Dannenberg, V.G. Zakrzewski, S. Dapprich, A.D. Daniels, M.C. Strain, O. Farkas, D.K. Malick, A.D. Rabuck, K. Raghavachari, J.B. Foresman, J.V. Ortiz, Q. Cui, A.G. Aboul, S. Clifford, J. Cioslowski, B.B. Stefanov, G. Liu, A. Liashenko, P. Piskorz, I. Komaromi, R.L. Martin, D.J. Fox, T. Keith, M.A. Al-Laham, C.Y. Peng, A. Nanayakkara, M. Challacombe, P.M.W. Gill, B. Johnson, W. Chen, M.W. Wong, C. Gonzalez, J.A. Pople, GAUSSIAN03, Revision B.01, Gaussian Inc., Pittsburgh, PA, 2003.
[32] A.R. Allouche, Gabedit, J. Comput. Chem. 32 (2011) 174–182.
[33] W.J. Geary, Coord. Chem. Rev. 7 (1971) 81–122.
[34] S. Chandra, A.K. Sharma, Spectrochim. Acta Part A 72 (2009) 851–857.
[35] M.A. Zayed, F.A. Nour El-dien, Djehad G. Mohamed, Spectrochim. Acta Part A 1 (2006) 216–232.
[36] S. Nigam, M.M. Patel, A. Ray, J. Phys. Chem. Solids 61 (2000) 1389–1398.
[37] S. Djebbar-Sid, O. Benali-Baitich, J.P. Deloume, J. Mol. Struct. 569 (2001) 121–128.
[38] S.Z. Jadhao, R.D. Rant, B.D. Saraf, Asian J. Chem. 17 (2005) 1059–1062.
[39] Y. Kaya, C. Icsel, V.T. Yilmaz, O. Buyukgungor, Spectrochim. Acta Part A 108 (2013) 133–140.
[40] A. Stanila, A. Marcu, D. Rusu, M. Rusu, L. David, J. Mol. Struct. 834 (2007) 364–368.
[41] O.B. Chanu, A. Kumar, A. Ahmed, R.A. Lal, J. Mol. Struct. 1007 (2012) 257–274.
[42] C.A.L. Becker, M.A.S. Biswas, J. Coord. Chem. 29 (1993) 277–286.
[43] B.N. Figgis, J. Lewis, R.G. Wilkins, Modern Coordination Chemistry, Interscience, New York, 1960 (Chapter 6).
[44] F.E. Mabbs, D. Collison, EPR of Transition Metal Compounds, Elsevier, Amsterdam, 1992. p. 379.
[45] V.S. Babu, A. Ramesh, P. Raghuram, R.R. Naidu, Polyhedron 1 (1982) 607–610.
[46] S. Djebbar-Sid, O. Benali-Baitich, J.P. Deloume, Polyhedron 16 (1997) 2175–2182.
[47] K. Kanmani Raja, D. Easwaramoorthy, S. Kutti Rani, J. Rajesh, Y. Jorapur, S. Thambidurai, P.R. Athappan, G. Rajagopal, J. Mol. Catal. A: Chem. 303 (2009) 52–59.
[48] S. Belaid, A. Landreau, S. Djebbar, O. Benali-Baitich, G. Bouet, J.P. Bouchara, J. Inorg. Biochem. 102 (2008) 63–69;
S. Belaid, A. Landreau, S. Djebbar, O. Benali-Baitich, G. Bouet, J.P. Bouchara, J. Inorg. Biochem. 102 (2014) 309–319.
[49] H.A.R. Pramanik, D. Das, P.C. Paul, P. Mondal, J. Mol. Struct. 1059 (2014) 309–319.
[50] B. Murphy, B. Hathaway, Coord. Chem. Rev. 243 (2003) 237–262.
[51] Ahmed M. Mansour, Inorg. Chim. Acta 394 (2013) 436–445.
[52] D.D. Perrin, Stability Constants of Metal-Ion Complexes: Organic Ligands, Pergamon Press, New York, 1979.
[53] S. Djebbar, O. Benali-Baitich, M. Khan, G. Bouet, Synth. React. Met.-Org. Chem. 27 (1997) 1219–1233.
[54] N. Tidjani-Rahmouni, S. Djebbar, N. Chenah, O. Benali-Baitich, Synth. React. Met.-Org. Chem. 29 (1999) 979–994.
[55] E. Pereira, L. Gomes, B. de Castro, Inorg. Chim. Acta 271 (1998) 83–92.
[56] S.K. Sengupta, O.P. Pandey, B.K. Srivastava, Trans. Met. Chem. 23 (1998) 349–353.
[57] A. Rohaya, A. Abdul Manaf, A. Dand, Life Sci. 76 (2005) 1953–1964.
[58] M. Tümer, D. Ekinci, F. Tümer, Spectrochim. Acta Part A 67 (2007) 916–929.
[59] R.R. Gupta, M. Kumar, V. Gupta, Heterocyle Chemistry II. Five-Membered Heterocycles, vol. XI, Springer-Verlag, Berlin, 1999. p. 638.
[60] G.W. Gokel, Int. Cong. Ser. 1304 (2007) 1–14.